Title
Lipid-Like Material as the Source of the Uncharacterized Organic Carbon in the Ocean?

Journal
Science, 299(5608)

ISSN
0036-8075

Authors
Hwang, Jeomshik
Druffel, Ellen RM

Publication Date
2003-02-07

DOI
10.1126/science.1078508

19. A. W. Tudhope *et al., Science* **291**, 1511 (2001).
20. It has been suggested that orbitally driven changes in insolation can modulate ENSO (*48*). We do not pursue this issue here, because our purpose is to understand whether reduced or absent ENSO is an inherent, permanent feature of warm climates. Our results do not exclude the possibility that cyclical modulation of ENSO on Milankovich time scales occurred also during the Eocene.
21. D. L. Royer, R. A. Berner, D. J. Beerling, *Earth Sci. Rev.* **54**, 349 (2001).
22. A. Timmermann *et al., Nature* **398**, 694 (1999).
23. G. A. Meehl *et al., J. Clim.* **13**, 1879 (2000).
24. M. Collins, *J. Clim.* **13**, 1299 (2000).
25. M. Blackmon *et al., Bull. Am. Meteorol. Soc.* **82**, 2357 (2001).
26. W. P. Chaisson, A. C. Ravelo, *Paleoceanography* **15**, 497 (2000).
27. M. A. Cane, P. Molnar, *Nature* **411**, 157 (2001).
28. M. Huber, L. C. Sloan, *Paleoceanography* **15**, 443 (2000).
29. P. N. Pearson *et al., Nature* **413**, 481 (2001).
30. D. P. Schrag, *Chem. Geol.* **161**, 215 (1999).
31. T. M. Rittenour, J. Brigham-Grette, M. E. Mann, *Science* **288**, 1039 (2000).
32. M. E. Mann, R. S. Bradley, M. K. Hughes, in *El Niño and the Southern Oscillation: Multiscale Variability and Global and Regional Impacts,* H. F. Diaz, V. Markgraf, Eds. (Cambridge Univ. Press, Cambridge, 2000), pp. 357–412.
33. B. L. Otto-Bliesner, E. C. Brady, *J. Clim.* **14**, 3587 (2001).
34. I.-S. Kang *et al., J. Clim.* **15**, 2791 (2002).
35. B. L. Otto-Bliesner, E. C. Brady, C. Shields, *Eos* **83**, (Fall Meet. Suppl.), abstract PP72B-03 (2002).
36. M. Huber, L. C. Sloan, *Geophys. Res. Let.* **28**, 3481 (2001).
37. Specifically, we compare values with the theoretical framework of (*11*). Our simulated values of easterly surface wind stress along the equator (~0.5 dyn cm^{-2}) and mean thermocline depth (~120 m) (fig. S5) place the Eocene simulation near the point marked "A" in their figure 4a, i.e., near modern values. The ENSO period associated with these conditions is ~5 years, matching those found in Eocene simulations and proxy records.
38. Today, maximum SST variability is found farther east, in the "Niño 3" (150°W to 90°W) and "Niño 3.4" (170°W to 120°W) regions. Given the different basin geometry in the Eocene simulation, a shift in location is not surprising. Today, the Niño 3.4 region brackets the zone where the Cold Tongue impinges on the Warm Pool. Thus, it strongly affects precipitation and hence diabatic heating and atmospheric circulation, making it the preferred region for studies of extratropical ENSO impacts. Precisely the same role is played in the Eocene simulation by our "Eocene Niño" region.
39. R. J. Allan, in *El Niño and the Southern Oscillation: Multiscale Variability and Global and Regional Impacts,* H. F. Diaz, V. Markgraf, Eds. (Cambridge Univ. Press, Cambridge, 2000), pp. 3–55.
40. M. Ghil *et al., Rev. Geophys.,* 10.1029/2000RG000092, 13 September 2002.
41. Lake sediments are affected by a number of seasonally varying factors, including temperature, insolation, snowmelt, runoff, and surface wind speed (*49*), whose interannual variations are recorded by changing layer thickness. Here, we concentrate on surface temperature and precipitation results.
42. M. Ripepe, L. T. Roberts, A. G. Fischer, *J. Sediment. Petrol.* **61**, 1155 (1991).
43. J. Mingram, *Palaeogeogr. Palaeoclimatol. Palaeoecol.* **140**, 289 (1998).
44. K. Fraedrich, *Tellus* **46A**, 541 (1994).
45. G. J. van Oldenborgh, G. Burgers, A. K. Tank, *Int. J. Climatol.* **20**, 565 (2000).
46. G. K. Vallis, *J. Phys. Oceanogr.* **30**, 933 (2000).
47. J. Bjerknes, *Mon. Weather Rev.* **97**, 163 (1969).
48. A. C. Clement, R. Seager M. A. Cane, *Paleoceanography* **15,** 731 (2000).
49. C. Morrill, E. E. Small, L. C. Sloan, *Global Planet. Change* **29**, 57 (2001).

50. M. H. acknowledges L. C. Sloan for mentorship and support by NSF ATM9810799 and the Packard Foundation. This study would not have been conducted without B. Otto-Bliesner and E. Brady having first demonstrated ENSO in their Cretaceous simulation. We authors also thank F. F. Jin, Z. Y. Liu, M. A. Cane, and S. G. Philander for sharing their ideas. The CCSM model, computer time, and graphics tools (NCAR Command Language, NCL) were provided through NCAR by the NSF. Support for both authors was provided by Dansk Grundforskningsfond through the Danish Center for Earth System Science.

Supporting Online Material
www.sciencemag.org/cgi/content/full/299/5608/877/DC1
Materials and Methods
Figs. S1 to S6
References

25 September 2002; accepted 2 January 2003

Lipid-Like Material as the Source of the Uncharacterized Organic Carbon in the Ocean?

Jeomshik Hwang and Ellen R. M. Druffel

The composition and formation mechanisms of the uncharacterized fraction of oceanic particulate organic carbon (POC) are not well understood. We isolated biologically important compound classes and the acid-insoluble fraction, a proxy of the uncharacterized fraction, from sinking POC in the deep Northeast Pacific and measured carbon isotope ratios to constrain the source(s) of the uncharacterized fraction. Stable carbon and radiocarbon isotope signatures of the acid-insoluble fraction were similar to those of the lipid fraction, implying that the acid-insoluble fraction might be composed of selectively accumulated lipid-like macromolecules.

Less than 40% of sinking POC collected below the euphotic zone can be molecularly characterized (*1*, *2*). The uncharacterized fraction constitutes an increasing proportion of POC with the depth at which it is collected, with the highest fraction in sedimentary organic carbon (*1*). What is the composition of the uncharacterized fraction and how is it formed?

One hypothesis for the formation of the uncharacterized fraction is abiological recombination of small molecules such as amino acids and carbohydrates produced by degradation of labile organic matter (*3*, *4*). This hypothesis has been challenged by results of ^{13}C and ^{15}N nuclear magnetic resonance (NMR) spectroscopy (*5*, *6*). A second hypothesis is that biologically produced refractory compounds are selectively accumulated whereas labile compounds are remineralized (*7*, *8*). Hydrolysis-resistant cell wall–derived material has been observed in recent and ancient sediments (*9*–*11*). A third hypothesis involves physical protection of organic carbon by refractory organic or inorganic matrices (*12*, *13*). A recent study explored solid-state ^{13}C NMR spectra of plankton and sinking POC collected at shallow and deep waters (*14*). The similarity of the spectra led Hedges *et al*. to suggest that the uncharacterized fraction was the same organic material produced biologically but was protected by mineral matrices or refractory biomacromolecules.

Department of Earth System Science, University of California Irvine, Irvine, CA 92697–3100, USA. E-mail: jeomshik@uci.edu (J.H.); edruffel@uci.edu (E.R.M.D.)

Biologically produced lipids, amino acids, and carbohydrates have distinct stable carbon isotope [$\delta^{13}C$ (*15*)] signatures because of the different physiological fractionation of carbon during their syntheses (*16*, *17*). Therefore, comparison of the $\delta^{13}C$ signature of the uncharacterized fraction with those of other organic fractions will provide insights as to its source(s). The radiocarbon isotope [$\Delta^{14}C$ (*18*)] signatures of all organic fractions are the same when measured in plankton from the surface water because they are fractionation-corrected. The overall signature changes when carbon with a different $\Delta^{14}C$ signature is incorporated and when the carbon is aged (*19*). Therefore, organic fractions that have similar sources, sinks, and residence times in the ocean will have similar $\Delta^{14}C$ signatures.

We measured $\delta^{13}C$ and $\Delta^{14}C$ values in sinking POC collected from a depth of 3450 m, at a site (Station M, 4100 m deep at the bottom, 34°50′N, 123°00′W) 220 km west of the California coast. We isolated biologically important compound classes: lipids, total hydrolyzable amino acids (THAA), total hydrolyzable neutral carbohydrates (TCHO), and a proxy of the uncharacterized fraction, the acid-insoluble fraction (*20*). The acid-insoluble fraction that remains after organic solvent extraction and acid hydrolysis accounts for ~70% of the uncharacterized fraction (*21*).

Sinking POC originates mainly from dissolved inorganic carbon (DIC) in surface waters, and it reaches the deep water on a time scale of months. Therefore, bulk sinking POC

is expected to have similar $\Delta^{14}C$ values to those of DIC in surface waters [40 to 80 per mil (‰) (*22*)]. The observed $\Delta^{14}C$ values of bulk sinking POC collected at a depth of 3450 m are lower than the expected values, which means that sinking POC acquired old carbon from other carbon reservoirs during the transit from the surface to the sampling depth. Thus, $\Delta^{14}C$ can be an indicator of diagenetic status of POC (i.e., how much old, degraded carbon is incorporated into sinking POC), assuming constant $\Delta^{14}C$ values of the source organic carbon.

The weight percentages of the characterizable fractions such as lipids, THAA, and TCHO are positively correlated with the $\Delta^{14}C$ values of bulk POC, whereas that of the acid-insoluble fraction is negatively correlated (Fig. 1). Thus, the higher the fraction of acid-insoluble organic carbon, the lower the bulk POC $\Delta^{14}C$ value.

The $\Delta^{14}C$ values of each organic fraction are plotted with respect to the bulk POC $\Delta^{14}C$ to show the relative amounts of old and new carbon (Fig. 2). The $\Delta^{14}C$ values of THAA and TCHO are similar to each other and close to those of surface water DIC. The $\Delta^{14}C$ values of lipids and the acid-insoluble fractions are similar to each other but are lower than those of THAA and TCHO. The $\Delta^{14}C$ values of lipids and the acid-insoluble fraction decrease at slightly higher rates than THAA and TCHO, making the difference between the two groups bigger as the bulk POC $\Delta^{14}C$ values decrease. The slopes of the lines imply that $\Delta^{14}C$ values will converge at or around the range of DIC $\Delta^{14}C$ in surface waters. The $\Delta^{14}C$ values of the four fractions from plankton collected at the same station were equal to the range of DIC $\Delta^{14}C$ (*23*). This indicates that all organic fractions of sinking POC originated from modern source(s) of carbon, but lipids and the acid-insoluble fraction acquired more old carbon than did THAA and TCHO.

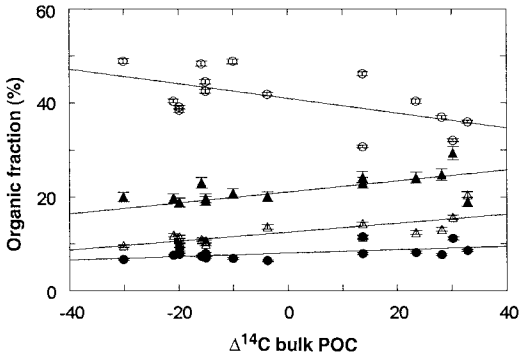

Fig. 1. Percent of each organic compound class (lipids, solid circles; THAA, solid triangles; TCHO, open triangles; acid-insoluble fraction, open circles) separated from several 10-day samples of sinking POC collected at a depth of 3450 m at Station M in the Northeast Pacific. The amounts of CO_2 of each compound class were measured manometrically after combustion and were compared to the organic carbon content measured with an element analyzer. The uncertainty is the larger value of 1σ of either the yield of standard material (replicate number >5) or a duplicate run of samples (3% for lipids, 5% for THAA, 3% for TCHO, and 1% for acid-insoluble fraction).

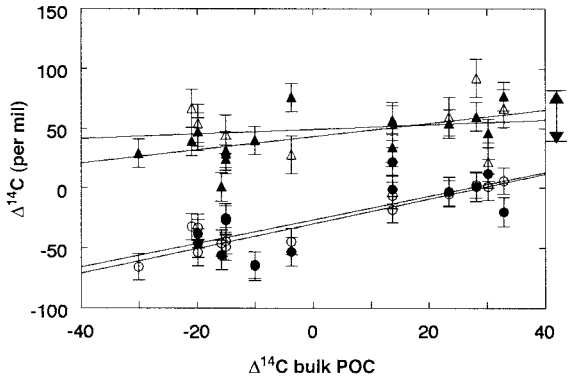

Fig. 2. The $\Delta^{14}C$ values of each organic compound class (symbols are as defined in Fig. 1). The black arrow by the right *y* axis indicates the range of DIC $\Delta^{14}C$ values in surface waters at Station M. The $\Delta^{14}C$ values are blank-corrected. We measured $\Delta^{14}C$ of an amino acid standard solution (mixture of 17 amino acids), D-glucose powder, and cod liver oil by the same methods as the samples. We compared these values with those of unprocessed standards to calculate the $\Delta^{14}C$ values of the blanks. The amounts of the blank were measured manometrically by combining five or six blanks together. Blanks were higher for THAA and TCHO, because there were more steps involved in their separation. The acid-insoluble fraction was not blank-corrected because the blank was smaller than 0.01 mg ($<$0.7% of the sample). The uncertainty is the larger value of 1σ of either standard material (replicate number >5) or duplicates of samples.

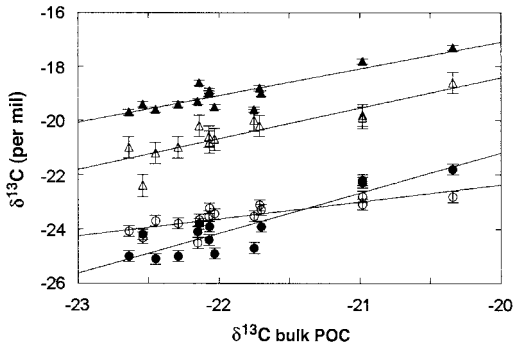

Fig. 3. The $\delta^{13}C$ values of each compound class (symbols are as defined in Fig. 1). The $\delta^{13}C$ values are blank-corrected by the same method as $\Delta^{14}C$. The uncertainty is the larger value of 1σ of either standard material or duplicates of samples.

The $\delta^{13}C$ values of lipids are 3 to 4‰ lower than those of THAA and TCHO (Fig. 3), as expected from physiological fractionation (*16*, *17*), but approximately equal to those of the acid-insoluble fraction. The differences in $\delta^{13}C$ between the organic fractions for each sample are constant even though $\delta^{13}C$ values in bulk POC samples vary by 2.5‰.

The constant differences in $\delta^{13}C$ between the acid-insoluble fraction and the other organic fractions provide constraints on its source(s). One possible scenario is that the acid-insoluble fraction is synthesized by the reaction between THAA and TCHO that are tightly bound with particles. However, the differences in $\delta^{13}C$ between the acid-insoluble fraction and THAA and TCHO (~4‰) argue against the degradation-recombination hypothesis of amino acids and carbohydrates for the formation of the acid-insoluble fraction. Two ^{13}C-enriched fractions cannot combine to form a ^{13}C-depleted fraction unless kinetic fractionation occurs during the chemical reactions. If kinetic fractionation occurs, one would expect ^{13}C to be enriched in remaining THAA and TCHO (*24*). However, the $\delta^{13}C$ values of the compound fractions were reported to remain constant for organic carbon of detrital aggregates, sediment floc, and sediment (0 to 20 cm) at the same location, and Wang *et al.* concluded that $\delta^{13}C$ signatures of each organic fraction were not affected by decomposition processes of organic matter (*23*).

The differences in $\delta^{13}C$ between the acid-insoluble fraction and THAA and TCHO argue against nonselective mineral protection as well. If the acid-insoluble fraction is simply the same material produced biologically as lipids, THAA, and TCHO, with the only difference that they are protected by mineral matrices, its isotopic signature should be similar to those of THAA and TCHO. Furthermore, treatment of the acid-insoluble fraction of POC with an HCl-HF solution to dissolve the mineral phases did not increase the extractable fraction of THAA and TCHO

significantly [<5% of total organic carbon (OC)] (*25*, *26*). However, our data do not argue against the hypothesis of selective mineral protection.

Another possibility is that the acid-insoluble fraction is protected lipids, THAA, and TCHO and contains a small fraction of old carbon [for example, old terrestrial carbon considering the location of the sampling site (220-km offshore)]. About 10% of the acid-insoluble fraction needs to be old carbon to explain observed low $\Delta^{14}C$ values (*27*). However, in order to explain the low $\delta^{13}C$ values of the acid-insoluble fraction, a much larger fraction (up to 50%) needs to be terrestrial carbon (*27*). Therefore, this mechanism cannot satisfy the $\delta^{13}C$ and $\Delta^{14}C$ results at the same time.

It is most likely that the major part of the acid-insoluble fraction is a selectively preserved part of organisms that is chemically different from amino acids and carbohydrates. Low $\Delta^{14}C$ values can be explained if the major portion of the acid-insoluble fraction is surface-originated fresh carbon and only a small fraction is older carbon that has aged and was incorporated into the particles. The source of the old carbon can be either dissolved organic carbon (DOC) or suspended POC. Resuspended sedimentary organic carbon will be old, but $\delta^{13}C$ values will be very similar to those of POC (*28*). Old carbon from eroded marine-origin bedrock is another possible source of old suspended POC (*29*).

The incorporation of old carbon into particles occurs more actively for lipids and the acid-insoluble fraction. Because lipids are hydrophobic and water-insoluble, they are more likely to be adsorbed to particles than are THAA and TCHO, most of which are water-soluble (*30*). The fact that the acid-insoluble fraction has similar $\Delta^{14}C$ values to those of lipids suggests that the two fractions have similar physicochemical properties. The similarity of $\delta^{13}C$ in lipids and the acid-insoluble fractions may suggest that both fractions are synthesized by similar biochemical pathways that are different from those for THAA and TCHO.

Our results suggest that the major portion of the acid-insoluble fraction is composed of lipid-like material that is biosynthesized by similar pathways to the extractable lipids, but somehow is resistant to organic solvents and acids. In fact, lipids are enriched in resistant parts of organisms such as membranes, spores, and cuticles (*4*). Selective preservation of these resistant lipids has been considered as one method of kerogen formation (*4*). The refractory cell wall–derived material of microalgae and bacteria, known as algaenans and bacterans, respectively, were found to make up a large part of kerogen and refractory organic carbon in sediments (*8*, *11*, *31*–*33*). They are, essentially, highly aliphatic lipids (i.e., a large number of carbon-to-carbon bonds) evidenced by release of *n*-alkane and *n*-alka-1-ene upon pyrolysis and by a high alkyl signal in ^{13}C NMR spectra. A network structure built up by cross-linking of long hydrocarbon chains was suggested as a protection mechanism against chemical attack (*9*). Considering that the mechanisms of lipid synthesis are similar in all organisms (*17*), these refractory macromolecules might be expected to have similar $\delta^{13}C$ signatures as those for the extractable lipids. The similarity of the nonhydrolyzable fraction and nonprotein alkyl carbon in chemical composition and abundance was observed in sediment from the continental margin of northwestern Mexico, and it was suggested that those components were compositionally similar to cell wall–derived algaenans (*33*). Even though these refractory lipid-like macromolecules have been studied only in sediments, selective accumulation of the lipids is likely to occur in the water column as the POC sinks. Selective accumulation of the refractory lipid-like material in the water column was evidenced by the observation that alkanes accounted for increasing fractions of the pyrolyzates of sinking POC as depth increased in the Equatorial Pacific (*34*) and the Mediterranean Sea (*35*).

Even though results of the ^{13}C NMR spectroscopy and direct temperature-resolved mass spectrometry on the samples from the Equatorial Pacific do not support the predominance of lipid-like material in sinking POC (*14*, *34*), the composition of sinking POC might vary depending on the local environment (*36*). The percentage of lipid in sinking POC in the Arabian Sea was twice as high as that in the Equatorial Pacific (*14*). Also, our sampling site can be influenced by laterally transported old carbon from the continental shelf or slope and from rivers in the California coast (*37*). Further study will be necessary to confirm if our observation is universal in the oceans. These results should provide important information to understand how organic carbon is preserved and removed from the carbon cycle in the ocean.

References and Notes

1. S. G. Wakeham, C. Lee, J. I. Hedges, P. J. Hernes, M. L. Peterson, *Geochim. Cosmochim. Acta* **61**, 5363 (1997).
2. J. I. Hedges *et al.*, *Org. Geochem.* **31**, 945 (2000).
3. J. I. Hedges, *Geochim. Cosmochim. Acta* **42**, 69 (1978).
4. B. P. Tissot, D. H. Welte, *Petroleum Formation and Occurrence* (Springer, Heidelberg, Germany, ed. 2, 1984), part II, chap. 2.
5. H. Knicker, A. W. Scaroni, P. G. Hatcher, *Org. Geochem.* **24**, 661 (1996).
6. M. McCarthy, T. Pratum, J. Hedges, R. Benner, *Nature* **390**, 150 (1997).
7. P. G. Hatcher, E. C. Spiker, N. M. Szeverenyi, G. E. Maciel, *Nature* **305**, 498 (1983).
8. E. W. Tegelaar, J. W. de Leeuw, S. Derenne, C. Largeau, *Geochim. Cosmochim. Acta* **53**, 3103 (1989).
9. J. W. de Leeuw, C. Largeau, in *Organic Geochemistry: Principles and Applications*, M. H. Engel, S. A. Macko, Eds. (Plenum, New York, 1993), pp. 23–72.
10. C. Flaviano, F. Le Berre, S. Derenne, C. Largeau, J. Connan, *Org. Geochem.* **22**, 759 (1994).
11. C. Largeau, J. W. de Leeuw, in *Advances in Microbial Ecology*, J. G. Jones, Ed. (Plenum, New York, 1995), vol. 14, pp. 77–117.
12. R. G. Keil, D. B. Montluçon, F. G. Prahl, J. I. Hedges, *Nature* **370**, 549 (1994).
13. R. A. Armstrong, C. Lee, J. I. Hedges, S. Honjo, S. G. Wakeham, *Deep-Sea Res. II* **49**, 219 (2002).
14. J. I. Hedges *et al.*, *Nature* **409**, 801 (2001).
15. The stable carbon isotope ratio is expressed as a relative ratio to the Pee Dee Belemnite standard, given by $\delta^{13}C = [(^{13}C/^{12}C)\text{sample}/(^{13}C/^{12}C)\text{standard} - 1] \times 1000$.
16. E. T. Degens, M. Behrendt, B. Gotthardt, E. Reppmann, *Deep-Sea Res.* **15**, 11 (1968).
17. M. J. DeNiro, S. Epstein, *Science* **197**, 261 (1977).
18. The $\Delta^{14}C$ value is the per mil deviation of the $^{14}C/^{12}C$ ratio relative to a standard. It is normalized to a $\delta^{13}C$ of –25‰ to remove isotopic fractionation effect. The half-life of ^{14}C is 5730 years. See (*38*).
19. E. R. M. Druffel, P. M. Williams, J. E. Bauer, J. R. Ertel, *J. Geophys. Res.* **97**, 15639 (1992).
20. Sinking POC was collected in a sediment trap equipped with an automatic sequencer set to collect samples at 10-day periods. The filtered POC (1 μm pore size) was dried at 50°C, ground, and stored in a freezer until analysis. The sample was cavitated with an ultrasonicator in a 2:1 volume/volume mixture of methylene chloride:methanol, and then was centrifuged. The extraction was repeated four times, and the combined supernatant was used as the lipid extract. Roughly half (weighed) of the residue was hydrolyzed for total hydrolyzable amino acids (THAA) (6 M HCl under N_2 gas for 19 hours) and the other half for total hydrolyzable neutral carbohydrates (TCHO) (2 hours in 72% H_2SO_4, then 3 hours in 0.6 M H_2SO_4). The hydrolyzates were eluted through ion exchange columns for the separation of THAA and TCHO. The organic carbon left after THAA extraction was used for the acid-insoluble fraction. Each organic carbon extract was acidified with 1 ml of 3% H_3PO_4, dried under vacuum, and combusted at 850°C for 2 hours with CuO and silver foil in a sealed tube. The resultant CO_2 was graphitized at 600°C on a Co catalyst. The $\Delta^{14}C$ measurements were performed at either the National Ocean Sciences Accelerator Mass Spectrometry Facility (NOSAMS), Woods Hole Oceanographic Institution (WHOI), or the Center for Accelerator Mass Spectrometry (CAMS), Lawrence Livermore Laboratory (LLNL). For a detailed description of the method, see (*23*).
21. The percentage was calculated from the ratio of the acid-insoluble fraction to the uncharacterized fraction that is the difference between the total organic carbon and the characterized fractions (lipids, THAA, and TCHO).
22. C. A. Masiello, E. R. M. Druffel, J. E. Bauer, *Deep-Sea Res. II* **45**, 617 (1998).
23. X.-C. Wang, E. R. M. Druffel, S. Griffin, C. Lee, M. Kashgarian, *Geochim. Cosmochim. Acta* **62**, 1365 (1998).
24. Y. Qian, M. H. Engel, S. A. Macko, *Chem. Geol.* **101**, 201 (1992).
25. J. Hwang, unpublished data.
26. After the extraction of lipid and acid-soluble fractions, the acid-insoluble fraction was treated with HCl-HF solution (5 ml of 1.5 M HCl and 5 ml of 50% HF) for 24 hours at room temperature, then was dried completely to remove HF. The extraction of lipids and acid-soluble fractions was performed on the demineralized fraction.
27. The fraction of old carbon was calculated by a mass-balance equation assuming that the acid-insoluble fraction is composed of lipids, THAA, and TCHO. Weighted averages of the lipids, THAA, and TCHO are 40‰ and –20.3‰ for $\Delta^{14}C$ and $\delta^{13}C$, respectively. The observed values of the acid-insoluble fraction are –23‰ and –23.5‰ for $\Delta^{14}C$ and $\delta^{13}C$, respectively. Assuming –500‰ and –27‰ for $\Delta^{14}C$ and $\delta^{13}C$ of terrestrial carbon, respectively, the percentage of terrestrial carbon (f) can be calculated by $40 \times (1 - f) + (-500) \times f = -23$

(f = 0.12 for $\Delta^{14}C$); –20.3 × (1 – f) + (–27) × f = –23.5 (f = 0.48 for $\delta^{13}C$).
28. R. M. Sherrell, M. P. Field, Y. Gao, *Deep Sea Res. II* **45**, 733 (1998).
29. C. A. Masiello, E. R. M. Druffel, *Global Biogeochem. Cycles* **15**, 407 (2001).
30. S. M. Henrichs, *Mar. Chem.* **49**, 127 (1995).
31. T. Eglinton, *Org. Geochem.* **21**, 721 (1994).
32. A. Garcette-Lepecq, S. Derenne, C. Largeau, I. Boulouba ssi, A. Saliot, *Org. Geochem.* **31**, 1663 (2000).
33. Y. Gélinas, J. A. Baldock, J. I. Hedges, *Science* **294**, 145 (2001).
34. E. C. Minor, S. G. Wakeham, C. Lee, *Geochim. Cosmochim. Acta*, in preparation.
35. S. Peulvé, J. W. de Leeuw, M.-A. Sicre, M. Baas, A. Saliot, *Geochim. Cosmochim. Acta* **60**, 1239 (1996).
36. X.-C. Wang, E. R. M. Druffel, *Mar. Chem.* **73**, 65 (2001).
37. K. L. Smith, R. S. Kaufmann, R. J. Baldwin, A. F. Carlucci, *Limnol. Oceanogr.* **46**, 543 (2001).
38. M. Stuiver, H. A. Polach, *Radiocarbon* **19**, 355 (1977).
39. We thank S. Griffin for guidance in laboratory work and C. Masiello, X.-C. Wang, C. Lee, and A. Ingalls for discussion on the experiments; K. Smith, J. Bauer, D. Wolgast, R. Baldwin, R. Glatts, F. Uhlman, R. Wilson, and the crews of the R/V *New Horizon* for help with sample collection; S. Trumbore and S. Zheng for shared equipment; A. McNichol, R. Schneider, J. Hayes, and colleagues at NOSAMS, WHOI, and J. Southon and colleagues at CAMS, LLNL, for the $\Delta^{14}C$ measurement; A. Gagnon for the $\delta^{13}C$ measurement; M. McCarthy for discussion and review of the manuscript; and C. Lee, T. Komada, S. Beaupré, and an anonymous reviewer for helpful comments on the manuscript. Supported by the Chemical Oceanography Program of NSF and the University of California Office of the President (fellowship to J.H.).

17 September 2002; accepted 7 January 2003

Design and Chemical Synthesis of a Homogeneous Polymer-Modified Erythropoiesis Protein

Gerd G. Kochendoerfer,[1]* Shiah-Yun Chen,[1] Feng Mao,[1] Sonya Cressman,[1]† Stacey Traviglia,[1]‡ Haiyan Shao,[1] Christie L. Hunter,[1]§ Donald W. Low,[1] E. Neil Cagle,[1] Maia Carnevali,[1] Vincent Gueriguian,[1] Peter J. Keogh,[1] Heather Porter,[1] Stephen M. Stratton,[1] M. Con Wiedeke,[1] Jill Wilken,[1] Jie Tang,[1]‖ Jay J. Levy,[1]¶ Les P. Miranda,[1] Milan M. Crnogorac,[1] Suresh Kalbag,[1] Paolo Botti,[1]# Janice Schindler-Horvat,[1] Laura Savatski,[2] John W. Adamson,[2] Ada Kung,[1] Stephen B. H. Kent,[1] James A. Bradburne[1]**

We report the design and total chemical synthesis of "synthetic erythropoiesis protein" (SEP), a 51-kilodalton protein-polymer construct consisting of a 166-amino–acid polypeptide chain and two covalently attached, branched, and monodisperse polymer moieties that are negatively charged. The ability to control the chemistry allowed us to synthesize a macromolecule of precisely defined covalent structure. SEP was homogeneous as shown by high-resolution analytical techniques, with a mass of 50,825 ±10 daltons by electrospray mass spectrometry, and with a pI of 5.0. In cell and animal assays for erythropoiesis, SEP displayed potent biological activity and had significantly prolonged duration of action in vivo. These chemical methods are a powerful tool in the rational design of protein constructs with potential therapeutic applications.

Optimal performance of protein pharmaceuticals is primarily determined by an appropriate balance among specificity, potency, and pharmacokinetic properties. However, the inability to produce homogeneous posttranslationally or chemically modified recombinant proteins has hampered their optimization to date. Both natural and recombinantly produced glycoproteins occur in multiple glycoforms, and this heterogeneity is reflected in different potency and pharmacokinetic properties (*1*–*5*). Using conventional polymers such as polyethylene glycol for modification of recombinant proteins introduces heterogeneity both in the polymers attached and in the attachment sites, with a consequent variability in biological properties (*6*–*9*).

We envisioned that recent advances in the total chemical synthesis of proteins (*10*–*14*) and in the chemical synthesis of monodisperse polymers (*15*) could be exploited to address this problem through the design and synthesis of polymer-protein constructs of defined covalent structure. Such precise atom-by-atom control of the covalent structure provides a unique way to systematically correlate molecular structure with function and enables the fine-tuning of the biological properties of a target protein of pharmaceutical interest.

Here, we describe the design, total chemical synthesis, and biological activity of a monodisperse, polymer-modified macromolecule, synthetic erythropoiesis protein (SEP). SEP had comparable specific activity in vitro, but superior duration of action in vivo, relative to human erythropoietin (Epo), a natural glycoprotein hormone that regulates the proliferation, differentiation, and maturation of erythroid cells (*16*).

We designed SEP to be a potent effector of the Epo receptor and to have prolonged circulation lifetime. The target structure of SEP is shown in Fig. 1. SEP contains a 166-amino-acid polypeptide chain (Fig. 1A) similar to the sequence of Epo (*16*) but differs significantly in the number and type of attached polymers (*17*). In particular, two branched polymer moieties of a precise length and bearing a total of eight negative charges (Fig. 1B) were designed for site-specific attachment through an oxime bond to two noncoded amino acid residues [Lys^{24} (N^{ε}-levulinyl) and Lys^{126} (N^{ε}-levulinyl)] that were incorporated into the polypeptide chain. These sites correspond to two of the four glycosylation sites found in Epo. Each branched precision polymer was designed to have the following: (i) a chemoselective linker, (ii) a hydrophilic spacer consisting of one polymer repeat unit, (iii) a core structure with four branch points, (iv) a linear polymer with 12 repeat units attached to each branch point, and (v) a negative charge–control unit at the end of each linear polymer. These precision polymer moieties were envisioned to give the SEP molecule a large hydrodynamic radius and a net negative charge at physiologic pH for optimal potency and prolonged duration of action in vivo (*18*). We also hoped that the precision polymers would enhance stability by shielding the folded polypeptide chain from attack by proteolytic enzymes, and that it would reduce immunogenicity, while retaining full biological potency.

[1]Gryphon Therapeutics, 250 East Grand Avenue, Suite 90, South San Francisco, CA 94080, USA. [2]The Blood Research Institute, Blood Center of Southeastern Wisconsin, 8727 Watertown Plank Road, Milwaukee, WI 53226, USA.

*To whom correspondence should be addressed. E-mail: Gkochendoerfer@gryphonRX.com
†Present address: Department of Biochemistry and Molecular Biology, Faculty of Medicine, University of British Columbia, 2146 Health Sciences Mall, Vancouver, BC V6T 1Z3, Canada.
‡Present address: Diosynth RTP, Inc., 3000 Weston Parkway, Cary, NC 27513, USA.
§Present address: Applied Biosystems, 850 Lincoln Centre Drive, Foster City, CA 94404, USA.
‖Present address: Celera Genomics, 180 Kimball Way, South San Francisco, CA 94080, USA.
¶Present address: Midwest Biotech, 12690 Ford Drive, Fishers, IN 46038–1151, USA.
#Present address: GeneProt Inc., 2 Pré-de-la-Fontaine, 1217 Meyrin/Geneva, Switzerland.
**Present address: Departments of Biochemistry & Molecular Biology, and The University of Chicago, Chicago, IL 60637, USA.